Optimal Transmit Coil Design for Wirelessly Powered Biomedical Implants Considering Magnetic Field Safety Constraints

Erik Andersen D, Curtis Casados, Binh Duc Truong D, and Shad Roundy D, Member, IEEE

Abstract—This article presents an investigation on the optimal design of a transmit coil for a wireless power transfer system (WPTS) for biomedical implants with the goal of maximizing the magnetic flux density (B-field) at the location of the implant while not violating magnetic field exposure limits. Maximizing the B-field correlates to higher transferable electric power for certain WPTSs, such as those that use magnetoelectric receivers. While previous works have optimized the thermal efficiency, or system efficiency, to our knowledge no one yet has developed the procedure to optimize the transmitter to maximize the B-field subject to an imposed safety limit constraint for magnetic field exposure. In addition to this safety constraint, the optimal design of the transmitter is considered when the system geometry or the input current is constrained. Equations for determining the design parameters of an optimal solenoid transmitter are derived subject to constraints on either transmitter size or electric current. If a certain magnetic field strength is required, solutions to the size and current of the transmitter are presented, which allow the desired fields without violating the safety constraint. The mathematical model is experimentally validated, and a case study is described that illustrates the optimal design rules.

Index Terms—Biomedical implants, magnetoelectric (ME) transducer, optimization, safety constraints, wireless power transfer (WPT).

I. INTRODUCTION

HE energy storage unit takes up a significant portion of the device volume for most biomedical implants. For instance, the battery of a pacemaker can occupy 90% of its volume [1]. Additionally, although these batteries may last years, once they are depleted, a surgeon is required to remove and replace the expired device. This surgery carries a wide array of risks, including infection, bleeding, and allergic reactions to anesthesia [2]. Wireless powering of these devices eliminates the excess surgeries and allows for device miniaturization, which can allow more precision in device placement, greater comfort, and a better standard of living for the implantable device recipient.

Manuscript received February 23, 2021; revised May 21, 2021; accepted June 21, 2021. Date of publication October 6, 2021; date of current version October 13, 2021. This work was supported by the National Science Foundation under Grant ECCS-1651438. (Corresponding authors: Erik Andersen.)

The authors are with the Department of Mechanical Engineering, University of Utah, Salt Lake City, UT 84112 USA (e-mail: erik.andersen@utah.edu; casados.curtis@gmail.com; binh.d.truong@utah.edu; shad.roundy@utah.edu).

Color versions of one or more figures in this article are available at https://doi.org/10.1109/TEMC.2021.3104787.

Digital Object Identifier 10.1109/TEMC.2021.3104787

Previous research in wireless power transfer (WPT) has addressed wirelessly powering biomedical implants. The majority of these works use a two-coil near field inductive wireless power system [3]–[8], or a multi- (more than three) coil system [9]–[11]. The receive coil is implanted within the body and coupled with an external transmit coil. Most of these systems operate in the low-radio frequency (RF) region below 20 MHz, but some work has been done on higher RF frequencies [12]-[14]. Inductive wireless power systems operate most efficiently when the transmitter and receiver coils are of similar size and the mutual inductance, or coupling, is relatively high. As the size of implants continues to shrink, however, the receive coil will necessarily shrink with the following likely effects: the mutual inductance and coupling will fall; the size of the receive coil will become small compared to the implant depth; the size of the transmit coil will become large compared to the receive coil; and the optimal operating frequency will go up. An increase in frequency due to small size results in higher attenuation in human tissue which further reduces efficiency [15]. In addition, relevant safety standards [16]-[19] have more stringent constraints at higher frequencies. For example, according to [16], [17], the allowable magnetic flux density (B-field) at 100 kHz is 100 μT compared to 0.29 μT at 6.78 MHz. Therefore, there is an incentive to explore methods to achieve WPT with very small receivers that operate efficiently at lower frequencies.

Magnetoelectric (ME) transducers typically utilize a magnetostrictive material that is laminated with a piezoelectric material. ME transducers have recently been used as both transmit and receive antennas [20]-[22]. According to [23], for a given frequency, the characteristic wavelength of an ME antenna could be five orders of magnitude shorter than the electromagnetic wavelength, thus leading to more efficient energy transfer for small devices operating at low frequencies. This reduction occurs because the characteristic wavelength of an ME antenna is defined by its mechanical properties, while that of a typical coil antenna is determined by its electromagnetic properties. Comparing overall system efficiency of very small receiver coil-based wireless power transfer system (WPTS) to ME receiver-based WPTS is an area of active research [24]-[27]. The outperformance of one system over another has not been conclusively shown. However, ME receiver-based WPTS seems promising given recent work [24], [28].

The key concept of a ME WPTS is shown in Fig. 1. A ME transducer is utilized as a receiver, which converts a magnetic

0018-9375 © 2021 IEEE. Personal use is permitted, but republication/redistribution requires IEEE permission. See https://www.ieee.org/publications/rights/index.html for more information.

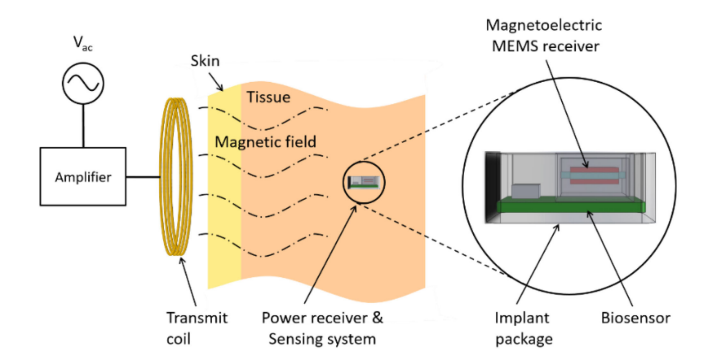


Fig. 1. Full system diagram of an ME transducer WPTS. The power generated by the receiver is positively correlated with the strength of the B-field. The system is loosely coupled, implying that the transmitter dynamics can be examined independent of the receiver.

wave produced by a transmit coil to electrical power to supply a biomedical implant. For a conventional resonant inductive coupling (RIC) WPTS, the magnetic energy is captured by a coil antenna based on the law of induction. However, different from an RIC configuration, an ME WPTS first transforms the magnetic energy to mechanical vibrations through the interaction of magnetostrictive material and the applied field. The vibrational kinetic energy is then converted to electrical form by a piezoelectric phase. The operation principle of an ME receiver was thoroughly investigated in [29]. The authors showed that the maximum possible power that can be delivered to a load $P_{\rm avt}$ is proportional to the square of the magnetic field amplitude H_0 . In particular,

$$P_{\text{avt}} = \frac{1}{8} \frac{\left(\Gamma_m H_0\right)^2}{b} \tag{1}$$

where Γ_m is the electrodynamic transduction factor and b is the mechanical coefficient. Γ_m is a function of the geometry and material parameters of the ME transducer. Meanwhile, b is solely dependent on the mechanical properties of the receiver side. For a given receiver structure implanted inside the human body, both Γ_m and b are determined ahead of time. Therefore, maximizing $P_{\rm avt}$ by optimizing H_0 generated at the implant location (which can be accomplished by an appropriate design of the transmitter geometry) is of great interest to study.

In any WPTS for biomedical implants, including ME and RIC, human safety considerations must be paramount. This safety concern is the reason that optimal design rules of other WPTS cannot be generally applied to WPTS that operate near or within the human body. The Federal Communications Commission, IEEE, and International Commission on nonionizing radiation protection (ICNRP) all have outlined safety limitations for WPT, particularly exposure to magnetic and electric fields [16]–[19]. The IEEE, for example, limits magnetic wave exposure to below 205 μ T for magnetic waves with frequencies between 3 kHz and 100 kHz [18]. For a ME WPTS, it is indicated that the optimal coil diameter that maximizes the transferred power depends upon the distance between the transmit coil and the ME receiver [30]. A bigger coil is more suitable for a large transfer range in general, and a smaller transmitter is preferable for a close distance. However, this argument may no longer hold when

subject to the safety standards and systems constraints, which the authors have not considered. Furthermore, universal rules to design an optimal transmitter have not been revealed yet.

In an implantable system, it is likely that the receiver is much smaller than the transmitter, and the distance between them is much larger than the size of the receiver. These unavoidable mismatches result in a weak coupling. Therefore, WPTSs used in biomedical applications typically have low transfer efficiency, which is usually less than 1%. For instance, the overall efficiency of the system reported in [29] was only 0.12%. Thus, the impedance reflected onto the transmit coil from the ME transducer can be disregarded. Additionally, if the operating frequency is low enough, the receiver is potentially much smaller than the electromagnetic wavelengths (e.g., at 1 GHz the EMF wavelength is 30 cm). These assumptions allow us to optimize the transmitter geometry without taking into account the appearance of the receiver; in other words, the transmitter can be considered purely as a magnetic field source.

The optimal design problem is to design the transmit coil to maximize the magnetic field at the location of the implant, subject to design constraints, while ensuring the magnetic field exposure is below the safety constraint at any point inside the human body. For instance, if the implant is 10 mm below the surface of the skin, one would seek to design a transmitter that maximizes the magnetic field at 10 mm below the surface of the skin while ensuring that the magnetic field at the surface of the skin (or anywhere else inside the body) is below the limits of the relevant safety standard. The idea behind this approach is that by determining the maximum achievable B-field at the implant, the designer can then design a receiving transducer to achieve the required power from this magnetic field. An alternative approach would be to first design the receiver, and then determine the required B-field that will provide adequate power. The analysis presented in this article is reversible such that the equations developed could also be used for this alternative approach. While this article focuses on ME WPTS, a similar analysis can be extended to an inductive coupling WPTS. In general, increasing the B-field at the receiver will increase the maximum power that can be delivered to the load. We also note that, when designing a RIC WPTS, other relevant parameters such as system coupling, resonance, coil quality factor, and impedance matching should be considered. However, these factors are out of the scope of this article.

With a focus on supplying low-power bioelectronics, we treat the actual power delivered to the load as the key metric of a ME WPTS. In this work, the central objective is to generalize design rules to attain a desired transmit coil. The questions on optimizing the overall transfer efficiency or designing a fully optimal system are left open for further investigation.

The rest of this article is organized as follows. The motivations and central objectives of the work are given in the Introduction. Relevant safety constraints are considered within the context of optimizing the transmitter design. Optimal transmitter designs considering only safety constraints are then explored. Further design constraints are then incorporated. These constraints include transmit coil size and placement constraints, and transmit current constraints. A case study is presented in which optimal transmit

coils (for ME-based WPTSs) are designed and experimentally validated. The article concludes with a discussion of generalized design principles and an optimal design process.

II. RELEVANT SAFETY STANDARDS

Due to the attenuation of electromagnetic fields within human tissue, the majority of WPTSs operate at low RF frequencies. At these frequencies, the reflection of the magnetic field on the human skin is negligible, and the magnetic properties of human tissue closely mirror those of free space [4], [31]. Two main international agencies currently govern the use of low frequency (below 10 MHz) nonionizing radiation: ICNRP and the International Committee on Electromagnetic Safety (ICES, which is a subsidiary of IEEE). Each agency has released its recommendations for safety standards [16]–[18]. While these safety standards were originally derived for environmental field safety, they are still applicable for WPT for medical applications.

The primary safety concerns with non-ionizing radiation exposure are RF shocks and burns, electrostimulation within the body, localized RF heating effects, surface heating effects, and whole-body heating effects. For frequencies below 5 MHz, RF shocks and electrostimulation are the primary concern. For frequencies of 100 kHz to 300 GHz, tissue heating becomes the primary concern. Given these adverse health effects, ICES and ICNRP have set exposure limits for both a controlled (occupational) environment and the general public.

For example, ICES has established "dosimetric reference limits (DRLs)" which are defined in terms of the electric field for RF shocks safety limit and specific absorption rates (SARs) for the thermal heating safety limit. The SAR safety limit in a controlled environment is 0.4 W/kg whole-body exposure and 10 W/kg for localized exposure. But, these basic restrictions can be challenging to measure and taxing to compute. Therefore, "exposure reference levels" or ERLs are introduced which are simpler and easier to measure. These are mostly defined in terms of magnetic field (B-field) exposure, although some ERLs are defined in terms of the electrical field exposure. ERL's are a more conservative safety estimate, a system complying with the ERLs will also comply with the DRLs and thus follow the safety regulations. The occupational/controlled-environment magnetic field exposure limits for both ICES and ICNRP as a function of frequency are presented in Fig. 2.

The allowable B-field dramatically decreases as the frequency of the magnetic field increases. The B-field is especially limiting at frequencies above 100 kHz. For a ME-based WPTS, the power of the receiver is proportional to the square of the B-field [30]. Thus, operating at frequencies below 100 kHz could result in higher safe power generation at the implant. Generating a B-field as close as possible to the allowable safety limit, depending on the chosen operating frequency, will maximize the available power at the implant.

For systems that operate at high RF frequencies (MHz – GHz range), the ERLs are too strict that it may be impossible to construct a useful WPTS that adheres to them. In these cases, directly calculating the DRL's (SARs) will offer better insight into the overall safety of the WPTS. However, we emphasize

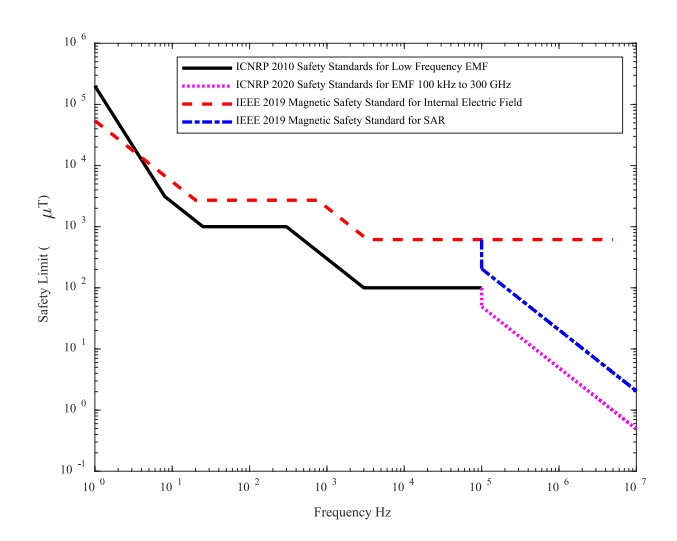


Fig. 2. ICNRP and IEEE ERLs for the B-field safety standards for human occupational/controlled-environment exposure as a function of frequency.

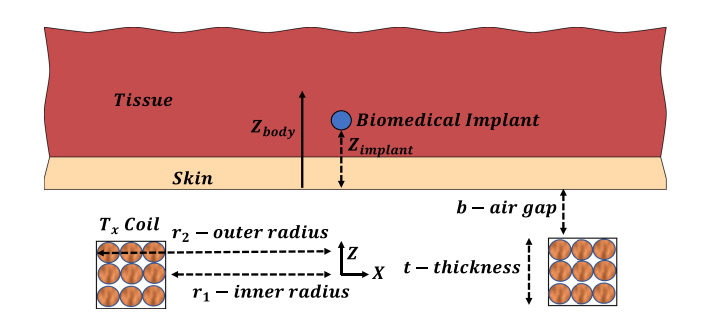


Fig. 3. Coil optimization parameters labeled with a cross-sectional view of the solenoid. The z-axis origin is in the middle of the solenoid coil, with an air gap between the coil and the body. The distance into the human body along the z axis is $Z_{\rm body}$ and the biomedical implant is located at a fixed distance of $Z_{\rm implant}$, measured from the skin, into the human body [36].

that ERLs can still be applied for RIC WPTS, as seen in a few works recently [32], [33]. On the contrary, the ERL limits are more appropriate and convenient for low-frequency devices, such as ME transducers, and will be utilized for all the analyses throughout this article.

III. TRANSMIT COIL OPTIMIZATION

It has been previously shown that the optimal electromagnetic geometry for maximizing the B-field at a point in space is a tapered cylinder; nevertheless, a solenoid design is 98.8% as effective as the optimally shaped electromagnet and is much easier to manufacture [34]. For a solenoid based transmit antenna, the B-field at a WPT receiver attached to a biomedical implant located inside a human body is dependent upon the following factors.

- 1) Distance into the body of the implant Z_{implant} .
- 2) Input current density J.
- 3) Coil thickness t.
- 4) Inner and outer radii r_1 and r_2 , respectively.
- 5) Gap between the transmit coil and the skin b [35].

The definitions of these parameters are shown in Fig. 3. The B-field is considered a function of current density, i.e., current

per area, instead of the actual current. This alternative is convenient to generalize the design of the solenoid transmitter. For example, a 10 turn solenoid with a 1 amp of RMS current is equivalent to a 1 turn solenoid with 10 A of RMS current in terms of the field generated, assuming the radii of the two solenoids are equal. However, the quality factor, *Q*-factor, of each transmit coil will be different, which can affect the overall transfer efficiency of the system. Nonetheless, the available power at the receiver of the two cases are identical since the corresponding B-field strengths at the receiver are equal in principle.

The objective is to maximize the power that can be transferred to an electrical load, which correlates to maximizing the B-field at the biomedical implant without violating a magnetic field safety limit. Hence, the constrained optimization problem becomes

$$max \ B(\mathbf{r}_1, \mathbf{r}_2, \mathbf{t}, \mathbf{b}, \mathbf{z}, \mathbf{J}) \ at \ z = \mathbf{Z_{implant}} + b$$

s.t. $B(\mathbf{r}_1, \mathbf{r}_2, \mathbf{t}, \mathbf{b}, \mathbf{z}, \mathbf{J}) < \mathbf{B_{safe}} \ \forall \ \mathbf{Z_{body}}.$ (2)

Solving the optimization problem in this form involves calculating the B-field produced by a solenoid which is given by

$$B = \frac{\mu}{4\pi} \iiint_{V} \vec{j} \, d\tilde{v} \wedge \frac{\vec{r} - \vec{r'}}{\left|\vec{r} - \vec{r'}\right|^{3}}$$
 (3)

where \vec{j} is the current density, and $\vec{r} - \overrightarrow{r'}$ is a space vector between a point where the magnetic field is calculated and a location inside the solenoid conductor.

Generally, for any point, (3) may necessitate evaluating elliptical integrals. Therefore, the problem was solved numerically using gradient-based optimization algorithms subjected to a safety limit constraint. Through this numerical optimization, several trends quickly emerge. As expected, there is always an ideal alignment between the solenoid and the biomedical implant, in which the receiver lies along the coil center axis. The optimal thickness t and the difference between the inner and outer radii, $r_2 - r_1$, are much smaller than the inner radius of the coil. The optimization pushes the design of the solenoid transmit coil to closely resemble a current loop. Using this insight, the governing equations for calculating the B-field for the solenoid along its z-axis can be simplified to

$$B = \frac{\mu}{4\pi} \frac{2\pi R^2 I}{(z^2 + R^2)^{\frac{3}{2}}} \tag{4}$$

where B is the B-field produced along the centerline at some distance z away by a current loop with a radius R, and current I, operating in some space with magnetic permeability μ . For human tissue, the magnetic permeability is equal to that of free space [37]. Equation (4) will be shown to be a good approximation for the solenoid magnetic field when compared with (3), COMSOL simulations, and an experimentally measured solenoid B-field in section IV on model validation (see Fig. 9 in particular).

A. Unconstrained Wireless Power Transmitter Optimization

The maximum achievable B-field at a point located $Z_{\rm implant}$ distance inside the body $B_{\rm max}$ can be represented as

$$B_{\text{max}} = \Gamma B_{\text{safe}}$$
 (5)

where $B_{\rm safe}$ is the maximum safe exposure limit, and Γ is a ratio less than or equal to one. If the B-field were completely uniform along the z-axis (see Fig. 3), Γ would be equal to 1 and $B_{\rm max}$ would be as high as it is allowed by the safety standard. If there are no constraints placed upon the size or power consumption of the transmit coil, the optimization process does in fact result in a transmit coil that emits a near-uniform magnetic field along the z-direction just under the imposed safety constraint (i.e., $\Gamma \approx 1$). In order to create this nearly uniform B-field, the transmit coil is tremendously large, with the radius of the coil much greater than the depth of the biomedical implant, and uses extremely high currents. However, this solution represents a highly idealized case that is unrealistic for practical design situations where available space and power are not infinite.

Therefore, this article will examine how the optimal design of the transmit coil for a WPT system is affected by both magnetic field safety constraints and either geometric/size constraints or power/current constraints. This investigation will provide useful insights into design rules for optimizing the achievable power at a biomedical implant without exceeding the magnetic field safety limit. The solutions to the constrained optimization problem differ significantly from the unconstrained case. The optimal design no longer produces a uniform magnetic field. The optimal B-field shape differs based upon the given constraints.

B. Geometrically Constrained Transmitter Optimization

Given the fact that the optimal transmit coil design resembles a current loop with the B-field described by (4), the geometric constraints consist of a constraint on the maximum radius of the coil R and the minimum and maximum distance that the coil can be placed from the skin b. If geometric constraints are imposed, the solution to the optimization problem yields an optimal coil design whose radius is equal to the geometric constraint: R is as large as the constraint will allow. As the minimum distance constraint is active, the air gap between the transmit coil and the skin should be minimal. Assuming that the transmit coil can be placed right at the skin (i.e., b=0), the required current in the optimal transmit coil is

$$I = B_{\text{safe}} \frac{2R}{\mu} \tag{6}$$

where the radius R of the coil is equal to the geometric constraint limit, and μ is the magnetic permeability of the human body, which can be considered to be identical to that of free space. Equation (6) is derived using (4) and solving for the current that would result in a magnetic field at the safety limit at z=0, or at the skin.

One interesting result of this optimization process is that the air gap should always be minimized. In other words, it is never beneficial to increase the air gap as it simultaneously requires an increase in the operating current of the transmit

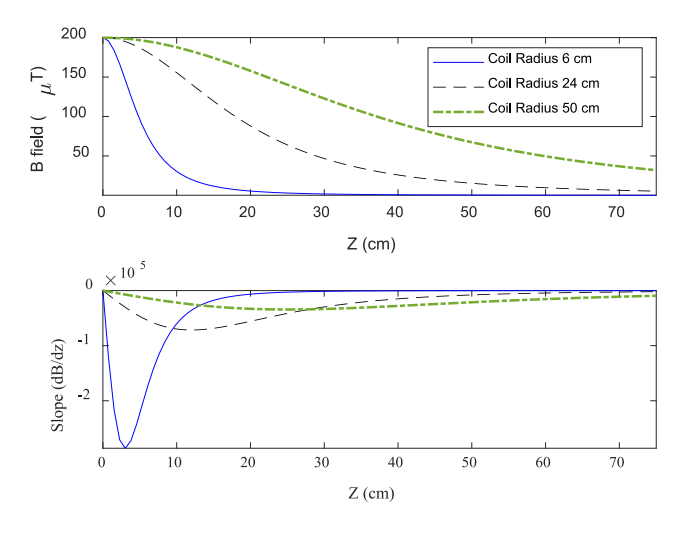


Fig. 4. B-field amplitude and its derivative with respect to the distance z for three transmitters with different radii using their optimal current. The shape of the B-field as well as $\frac{dB}{dz}$ is similar in all three cases. The slope of the B-field is always negative, and always initially becomes more negative (i.e., the curvature is negative) before flattening out [36].

coil to compensate for the B-field at the implant location. The justification for this result is seen by examining the shape of the B-field produced by a current loop. Taking the derivative of (4) with respect to z yields

$$\frac{dB}{dz} = -\frac{\mu}{4\pi} \frac{6\pi R^2 I}{(z^2 + R^2)^{\frac{5}{2}}} z.$$
 (7)

Equation (7) shows that the slope of the B-field is always negative, and the most significant drop in B-field occurs close to the transmit coil. This principle is indicated in Fig. 4, in which the B-field amplitude and its derivative in terms of the distance are presented for three coils with different radii. It should be noted that the corresponding optimal current of each coil is used. The B-field of the different sized coils falls at different rates depending on the radius of the coil. The smallest coil has a B-field with a high initial negative slope, while the largest coil B-field has a much lower initial slope. The slope of the B-field is always negative and initially becomes more negative before flattening out and approaches zero at large distances. It is impractical to operate in the area where the slope is level, since this property occurs at distances much larger than the radius of the coil and would require very high currents. As analyzed in the previous section, such a method can only be implemented when the coil geometry and input power are not constrained, which are unfeasible.

It is desirable to minimize the air gap as much as possible (ideally, b=0). However, a non-zero small air gap may be necessary for some realistic circumstances. For many large coils, the magnetic field near the coil windings is stronger than that in the coil center. Depending on the input current, this phenomenon could cause B-field strengths at a small space near the coil windings to exceed the safety limit. If these scenarios take place, (3) can also be used to find the distance at which the B-field no longer violates the safety standard. The obtained value can be considered as the minimum required air gap. Appendix A

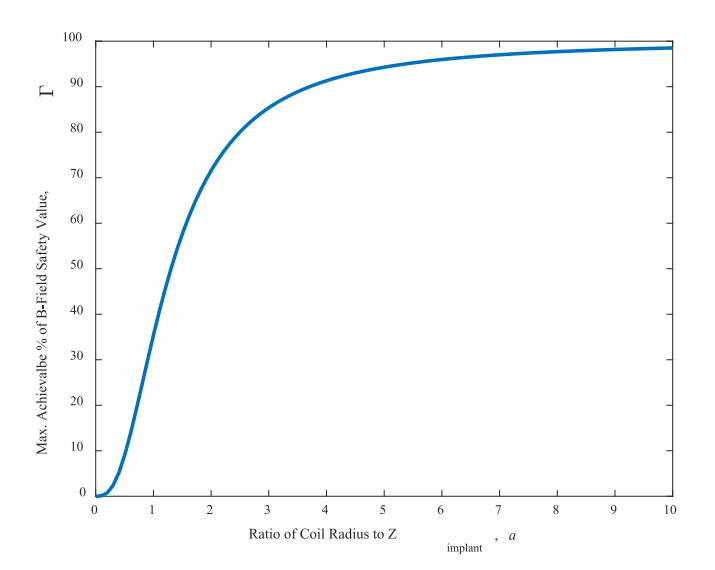


Fig. 5. Size constraint effects on maximum achievable B-field. The larger the allowable size of the coil relative to the implant depth, the higher the attainable B-field at $Z_{\rm implant}$ [36].

outlines how the optimal design rules are modified when a nonzero constraint on the air gap is essential.

The optimal design of the transmitter is a solenoid with its radius equal to the size constraint (i.e., maximum allowed), the air gap minimized to zero, and the excitation current is determined by (6). For this configuration, the maximum B-field at the implant $B_{\rm max}$ can be determined by solving (4) with $z=Z_{\rm implant}.$ Making use of (6) to define the B-field safety limit $B_{\rm safe}$ and referring back to (5), the ratio between $B_{\rm max}$ and $B_{\rm safe}$ can be derived as

$$\Gamma = \frac{B_{ ext{max}}}{B_{ ext{safe}}} = \frac{R^3}{\left(Z_{ ext{implant}}^2 + R^2\right)^{\frac{3}{2}}}.$$
 (8)

Furthermore, if the radius of the transmit coil is written in terms of a constant a multiplied by the implant depth

$$R = aZ_{\text{implant}}.$$
 (9)

Equation (10) is reduced to

$$\Gamma = \frac{\boldsymbol{a}^3}{(1+\boldsymbol{a}^2)^{\frac{3}{2}}}.$$
 (10)

If the geometric radius constraint is framed in this sense (i.e., the maximum allowable coil radius is a times the depth of the implant), then (10) can be utilized to compute the maximum possible fraction of the safety limit for a given radius constraint. A demonstration of (10) is shown in Fig. 5. As a summary, (10) defines the maximum achievable magnetic field for any implant depth solely as a function of the geometric constraint.

Additionally, this process is reversible. If a particular magnetic field strength is required at the biomedical implant (8) or (10) can be used to determine the minimum size coil that will produce the required magnetic field without violating the safety limit. For example, if the safety limit is 200 μ T (IEEE standard for a 100 kHz magnetic field), and the necessary B-field for successful wireless powering of the implant is 150 μ T (i.e.,

 $\Gamma=0.75$), then the transmit coil radius must be at least equal to 2.2 times the depth of the biomedical implant.

C. Current Constrained Optimal Transmitter

Attention is now turned to the case in which the electrical current serves as the design constraint, rather than the coil radius and placement (i.e., geometry). The goal of the optimization problem is to find the current and radius combination that maximizes the B-field at the implant. As we expected, it is always the case that the optimal current is at the constraint, which is the maximum allowed. If we assume that the coil is placed as close to the skin as possible, the coil radius becomes the only remaining design parameter. The optimal coil radius is dependent on the given current constraint, the magnetic field safety limit, and the depth of the biomedical implant.

When performing the optimization algorithm, subject to the current and safety constraints, we observed an important phenomenon. The optimal radius of the transmitter was either constant or a linear function of the implant depth Z_{implant} . This behavior appears for any given set of the current constraint and safety limit. The distance at which the optimal radius changes its tendency is referred to as critical distance $Z_{\rm crit}$ as defined in Fig. 6(a). The numerical results are illustrated in Fig. 6(b), which shows the optimal coil radius in terms of Z_{implant} for different current constraints. It is essential to point out that $Z_{
m crit}$ obtains the value of Z_{implant} at which the constant-optimalradius line (parallel with the x-axis) intersects with the function $R = \sqrt{2} Z_{\text{implant}}$. In addition, Z_{crit} is dependent upon the current and B-field safety constraints. For instance, $Z_{\rm crit}=1.1$ cm for a current constraint of 5 A and $Z_{\rm crit}=3.3$ cm for 15 A. The magnetic field safety limit is 200 μT for both examples.

As shown in Fig. 6(b), if $Z_{\rm implant} \geq Z_{\rm crit}$, the optimal radius is

$$R_{\rm opt} = \sqrt{2} Z_{\rm implant}.$$
 (11)

At the critical point $Z_{\rm crit} = Z_{\rm implant}$ the optimal radius in (14) can be rewritten as

$$R_{\rm opt} = \sqrt{2} Z_{\rm crit}.$$
 (12)

Furthermore, when $Z_{\rm implant} \leq Z_{\rm crit}$, the optimal radius of the transmit coil is a constant (independent of $Z_{\rm implant}$). Therefore, the relation in (12) holds for all $Z_{\rm implant} \in [0, Z_{\rm crit}]$. In this range of the implant depth, $R_{\rm opt}$ is dependent on both the current constraint and the safety limit. By substituting the electrical current constraint $I_{\rm max}$ into(6), $R_{\rm opt}$ is obtained as follows:

$$R_{\rm opt} = \frac{\mu I_{\rm max}}{2B_{\rm safe}}.$$
 (13)

From (13) and (12), the closed form expression of the critical distance is given by

$$Z_{\text{crit}} = \frac{1}{2} \frac{\mu I_{\text{max}}}{B_{\text{refo}} \sqrt{2}}.$$
 (14)

It is important to note that $Z_{\rm crit}$ is not an independently chosen parameter, but rather is a function of the magnetic field safety limit and current constraint. $Z_{\rm crit}$ plays an essential role in the

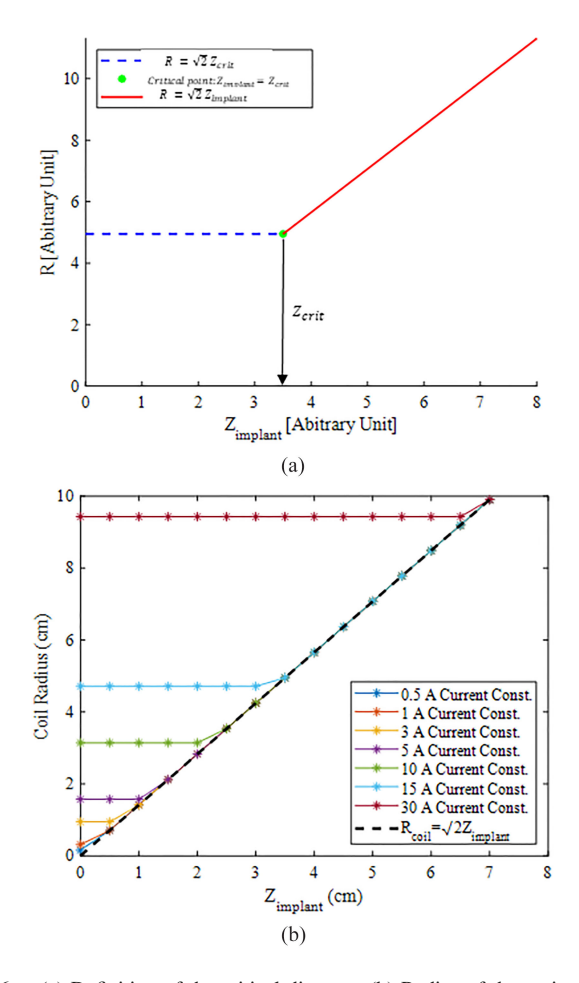


Fig. 6. (a) Definition of the critical distance. (b) Radius of the optimal coil design in terms of implant depth for different current constraints. The magnetic field safety limit is held constant at 200 μT for all cases. For shallow implant depths ($Z_{\rm implant} < Z_{\rm crit}$), the transmit coil radius is constant for a given case. Once the implant depth is equal to $Z_{\rm crit}$, the radius increases linearly at the same rate for all cases, independent of the current and magnetic field safety constraints [36].

design process as it represents the distance at which the optimal design path of the transmitter changes.

In order to further gain insight into the origins of (11) and (12), we now consider these two cases analytically. In either circumstance, the optimal radius is equal to a distance multiplied by the square root of two. The reason for this fact can be examined by looking at the optimization problem with and without the safety concern. If there is no magnetic field safety limit, but only a current constraint, the optimization problem is simplified. Once again, the maximum B-field occurs when the current constraint is active. The optimal radius can be found by setting the derivative of (4) with respect to the radius R equal to zero, which yields

$$\frac{dB}{dR} = \frac{2\pi 10^{-7} I \left(2Rz^2 - R^3\right)}{\left(R^2 + z^2\right)^{\frac{5}{2}}} = 0.$$
 (15)

Solving (15) for R gives

$$R = \sqrt{2} z. \tag{16}$$

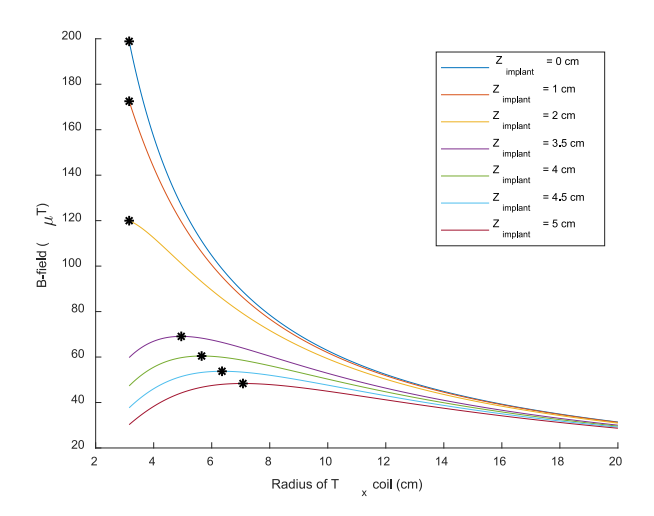


Fig. 7. B-field plotted at different distances inside the human body $Z_{\rm implant}$, vs the radius of the transmit coil. The max B-field is marked on each curve. The smallest allowable coil radius is 3.16 cm, any smaller and the safety limit of 200 μ T at the skin would be violated. For all distances less than $Z_{\rm crit}$, 2.2 cm in this case, the max B-field occurs with a coil radius equal to 3.16 cm. For distances greater than $Z_{\rm crit}$, the max B-field occurs at a unique transmit coil radius dependent upon the location of the implant.

With the goal of maximizing the B-field at $z = Z_{\text{implant}}$, (16) is identical to (11) In that sense, (11) is equivalent to the optimal design of a current constrained transmitter without regard to the magnetic field safety limit, or if the magnetic field safety constraint is not active for a given system. It should be noted that the solution to (11) results in a unique radius for every different implant depth Z_{implant} . However, using (11) for all current constrained WPTS could violate the safety constraint in some circumstances, specifically at shallow depths. In these situations, there is a single optimal coil design for which the current is equal to the constraint and the radius of the coil is set such that the B-field is just under the safety limit at the skin. Equation (12) shows the optimal coil radius for this scenario. In this regard, Z_{crit} represents the distance at which the safety constraint switches from being active at the skin to be being non active.

It is useful to analyze the two different modes of operation in the investigation of the optimal coil radius by looking at a specific example. These modes are illustrated in Fig. 7, in which the current constraint is set at 10 A, and the maximum achievable B-field B_{max} is expressed as a function of the coil radius for different implant depths starting at $Z_{\rm implant} = 0$ (i.e., the implant is right at the skin). The safety constraint for this example is $200 \,\mu\text{T}$, $B_{\text{safe}} \leq 200 \,\mu\text{T}$. We note that if $Z_{\text{implant}} = 0$, the safety limit is reached for a coil radius of 3.16 cm. The B-field at the location of the implant, which is also at the surface of the skin, is 200 μ T ($\Gamma = 1$). As the depth of the implant becomes larger $B_{\rm max}$ decreases. Taking $Z_{\rm implant} = 1~cm$ for example, $B_{\rm max} =$ $173~\mu$ T. The optimal radius is still 3.16 cm since the magnetic field at the surface of the skin is still 200 μ T ($\Gamma = 0.875$), and any further decrease in coil radius would violate the safety constraint. However, if Z_{implant} is between 2 and 3.5 cm, the shape of the $B_{\rm max}$ curve changes. The optimal coil radius is now not only a function of the safety limit, but also a function of the implant

TABLE I EXPERIMENTAL OPTIMAL COIL PARAMETERS

Coil Radius	Number of	Wire	Current
 	Turns	Diameter	(RMS)
5.65 cm	9	1.291 mm	15 A
! ! !		(16 AWG)	
7.78 cm	9	1.291 mm	15 A
		(16 AWG)	

depth. This is due to the fact that the safety constraint is no longer active. In other words, the coil radius that results in the highest $B_{\rm max}$ does not produce a B-field at or beyond the safety limit anywhere within the body. For this example, the delineation between these two regimes, the safety constraint being active or not active, is at $Z_{\rm implant}=2.2$ cm, which distance is equal to $Z_{\rm crit}$ calculated using (14).

If a certain Γ or B-field at the implant is required, the process of finding the minimum current is identical to the procedure outlined in the previous section, since the minimum coil radius that provides a certain Γ also requires the least current. The desired coil radius can be calculated using (10) and the corresponding minimum current can be achieved by (5).

IV. MODEL VALIDATION AND CASE STUDY

In order to validate the mathematical models and design insights, two transmit coils were constructed whose parameters are given in Table I. In order to reduce environmental impacts on the B-field, the coils were mounted to a support that raised the coils 21 cm above the lab table. The support was made of customized three-dimensional (3-D) printed ABS plastic parts and aluminum beams and screws, as depicted in Fig. 8.

Each transmitter was supplied with 15 A of RMS current at 80 kHz, and the B-field along each centerline axis was measured and recorded using a MC110A magnetic field sensor (Magnetic Sciences Inc.). A frequency of 80 kHz was chosen to minimize sensor error in the measurements. The sensor was mounted on a modified 3-D printer which moved the sensor along the centerline of the coil's z-axis, as seen in Fig. 8. Magnetic field readings were taken every 2 mm. In Fig. 9, the experimentally measured B-field using the MC110A sensor, the simulated B-field using both (3) (numerical) and (4) (analytical) solved using MATLAB, and a COMSOL 5.3a simulation for each coil along its z-axis are compared. In the COMSOL simulation, the copper wire coils were modeled in air using the dimesions given in Table I in a 2-D axisymmetric model. Using the magnetic field physics solver with a "finer" mesh, the coils were excited by 15 A RMS current at 80 kHz and the magnetic field was measured along the coils centerline.

The experimental data match closely with those predicted by equations and simulations for both coils, generally within 5% error. The error of the MC110A sensor is listed at 5%, which explains these small discrepancies. The close agreement between the mathematical models and the COMSOL finite element analysis gives confidence in the assumption that (4) is valid for determining the B-field for solenoid transmitter.

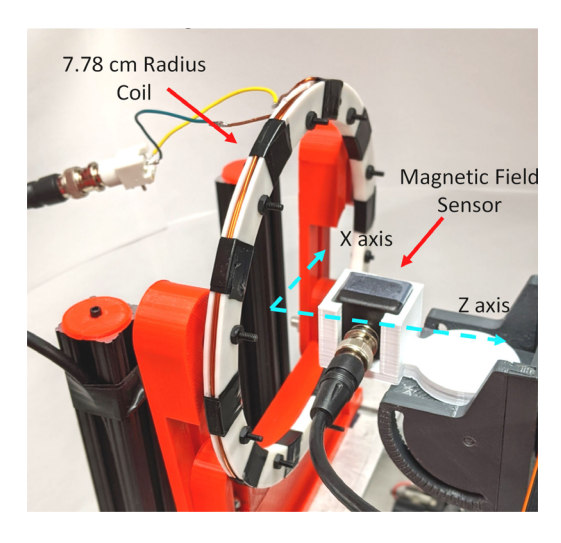


Fig. 8. 7.78 cm radius solenoid coil attached to the experimental setup. The setup consists of aluminum supports and screws as well as ABS plastic. These materials were selected because of their neutral magnetic properties. Two different transmit coils were constructed with different radii and each coils' B-field was experimentally validated.

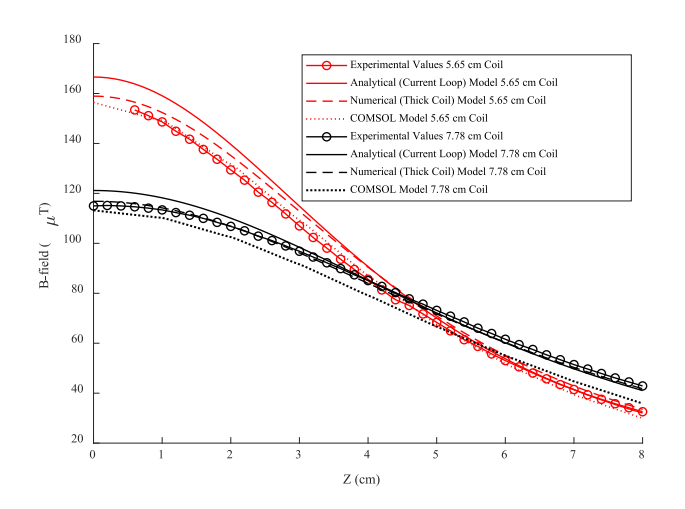


Fig. 9. Experimentally measured B-field field using the MC110A magnetic field sensor, simulated B-field data using COMSOL, the analytical solution to the B-field of a current loop along its centerline, and a thick solenoid coil B-field numerical approximation versus distance into the human body for the 7.78 cm coil. The measured experimental data closely follows the simulated data.

This lends creditability to optimization rules that were derived in the previous sections using these models. The experiments were conducted in air since the magnetic properties of tissue are almost identical to that of free space at low frequencies [4], [9], [38].

The optimal design rules for transmit coils proposed in this article can be explored through a case study, in which the implant distance $Z_{implant}$ is 3, 4, and 5.5 cm. The transmitter has both size and power constraints. In particular, it must be capable of being handheld (coil radius under 20 cm) and has a current limit of 15 A(RMS). The operating frequency of the transmitter is (arbitrarily) chosen as 73 kHz and, as such, the B-field cannot exceed the IEEE safety limitation of $200~\mu T$. At low frequencies, the attenuation of an applied B-field due to traveling through human tissues is negligibly small. Additionally, it is assumed that the coil can be placed right at the skin.

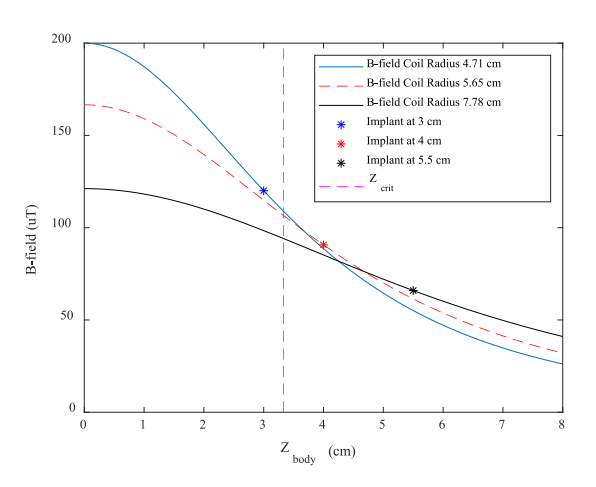


Fig. 10. Simulated B-field using the analytical model in (4) as a function of the distance into the body for three coils optimized around different implant depths. The optimally designed coil gives a greater B-field at its own implant distance in comparison with the other two coils. At any distances, all three coils produce a B-field that is under the safety limit of 200 μ T.

With the B-field safety limit given, $B_{\rm safe} \leq 200~\mu{\rm T}$, the next step is to determine if the size or current is the limiting constraint. We first set the radius equal to the constraint $R=20~{\rm cm}$, and use (6) to calculate the required current, which leads to $I=67.3~{\rm A}$. Meanwhile, the design constraint is 15 A, hence the current constraint will be the limiting factor. Now (11)–(14) are utilized to determine the optimal radius of the transmitter. Solving (14) for this system yields a $Z_{\rm crit}$ of 3.33 cm, meaning that the first implant at 3 cm is located at a distance less than $Z_{\rm crit}$ while the second and third implant distances, 4 and 5.5 cm, are greater than $Z_{\rm crit}$. Setting $I=15~{\rm A}$ and using (12), the optimal radius for the first implant is 4.71 cm. For the latter two implants, (11) results in the optimal radii of 5.66 and 7.78 cm, respectively.

Using (4), the B-field for each of the three solenoid coils with the aforementioned radii was presented in Fig. 10. The smallest coil produced the highest B-field for any point up to $Z_{\rm crit}$, including the first implant depth of 3 cm. We note that the safety constraint is active only for the smallest coil for which $Z_{\rm implant} < Z_{\rm crit}$. Beyond 3 cm, the coils with the larger radii supplied higher B-fields at the larger implant distances. In particular, the B-field of the largest coil (7.78 cm radius) is the greatest at the 5.5 cm distance. The coil with the 5.65 cm radius produced the highest B-field at the implant distance of 4 cm. However, it generated a B-field smaller than that of the 4.71 cm radius coil for distances under $Z_{\rm crit}$ and the 7.78 cm coil for distances near the 5.5 cm implant. All coils maintained a B-field under the safety limit of 200 μT at every point along the z-direction. It is noted that the coils in Table I are the optimally designed coils for implants located at 4 and 5.5 cm. All three coils were built and experimentally shown that they maximized the B-field at their respective implant depths. As mentioned in Section II, at low frequencies, the electric field is usually the limiting constraint. However, since the considered system does not violate the ERLs limit (defined in terms of the magnetic field), it does not violate the electric field DRL either [18]. This result was verified in a COMSOL simulation of the coil's electric field.

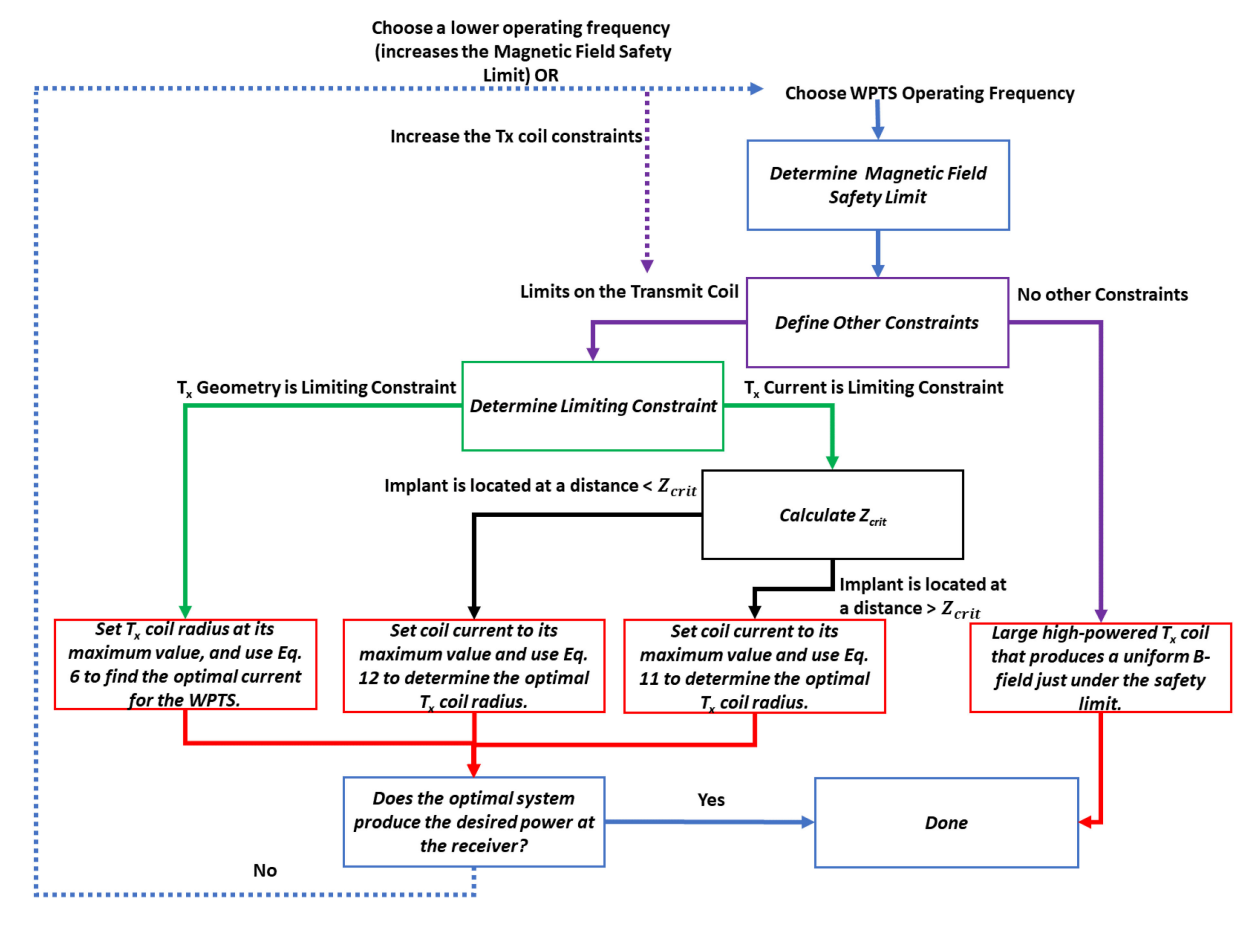


Fig. 11. Flow chart illustrating the three step design process for optimal transmit coil design.

V. DESIGN CONSIDERATIONS AND DESIGN PROCESS

The optimal design study and case study lead to the following three step generalized design process, which is illutrated graphically in Fig. 11.

- 1) Define system constraints
 - a) Determine desired operating frequency of the WPTS based on system parameters and operating requirements. Based on chosen frequency, find the magnetic field safety limit according to the chosen standard, IEEE or ICNRP [16]–[18].
 - b) Define either the geometric and/or current constraints for the WPTS based on the requirements of the operational scenario.
- 2) Determine limiting constraint and set the corresponding design parameter at the maximum allowable value
 - a) If there is only one constraint, that constraint is the limiting constraint.
 - b) If there are multiple constraints, set the radius equal the design constraint and calculate the required current using (6). If that current is below the current constraint, the radius constraint is limiting. Otherwise, the current is the limiting constraint.
 - c) If there are no constraints other than the magnetic field safety limit, the optimal solution is to make a giant coil that produces a uniform B-field in the axial direction. This, however, is unlikely to be realistic.

- Solve for the optimal parameter(s) that are not the limiting constraint
 - a) In all cases, minimize the air gap between the transmit coil and the subject body. If the air gap cannot be zero or close to zero, see appendix for optimal design equations for a nonzero air gap.
 - b) If the transmit coil radius is the limiting constraint, use (6) to determine the required current. Use (4) to calculate the corresponding maximum achievable B-field at the implant $B_{\rm max}$.
 - c) If the current is the limiting constraint, use (14) to determine $Z_{\rm crit}$. If the implant is located a distance greater then $Z_{\rm crit}$, use (11), otherwise use (12) to calculate the coil radius. Again, use (4) to determine $B_{\rm max}$.

If there is no feasible solution (i.e., any design that meets geometric and/or current constraints does not produce a B-field at the implant that can provide the necessary power), the designer must loosen either the geometric or current constraints. An alternative possible solution would be to redesign the system for a much lower operating frequency at which there is a higher B-field safety limit.

The central objective of the article is to design a transmit coil to maximize the B-field at the implant location given safety, size, and current constraints. The idea behind this approach is that by determining the maximum achievable B-field, $B_{\rm max}$, at

the implant, the designer can then design a receiving transducer, especially the ME receiver presented in Section II, to achieve the required power from $B_{\rm max}$. An alternative method would be to first design the receiver, and then determine the required $B_{\rm max}$ that will provide adequate power. Under this scenario, (8) can be used to optimize the coil geometry and (6) can be utilized to determine the required current to achieve the desired $B_{\rm max}$.

Additionally, the design process introduced in this work assumes that the air gap b between the transmit coil and the skin can be minimized to be close to zero. This is because the maximum magnetic field for a WPTS for an implant always occurs when the air gap is zero or nearly zero. However, if there is a constraint on the system that does not allow the air gap b to be near zero, the equations derived in the previous sections can be adapted to maximize the B-field at the implant considering the non-zero air gap. The extended equations are explained in the appendix. The general design process above applies equally to both scenerios when the air gap is zero or non-zero.

In the interest of clarity, some important aspects of the transmitter have not been discussed here. The transmit coil will naturally be designed with copper wire with finite resistance that produces heat when current is applied. The generally recommended current density to avoid overheating of copper wire is between $5-6 \frac{A}{\text{mm}^2}$. Once the optimal radius and current of the transmitter is determined, the thickness of the coil should be adjusted such that the current density does not exceed this limit. Moreover, the required current could be lowered by using smaller wire gages and an increasing number of terms. Previous work has been done on the optimal techniques to construct solenoids consisting of multiturn wires [39]–[41]. Finally, the efficiency of the transmitter system has not been considered in this article. The goal here was to optimize the transmit coil geometry. However, in most circumstances it is also important to design the transmitter electronics to either maximize the system efficiency or minimize the transmitter power consumption for a given produced B-field. This includes designing high Q transmit coils, which could improve the efficiency of the system. Nonetheless, the key conclusions, and attendant optimal design process, still hold and can provide a useful design guide.

VI. CONCLUSION

The optimal design for a transmit coil to power biomedical implants while staying below a magnetic field safety limit depends heavily on the system constraints (such as, B-field safety constraint, transmit coil geometry, and current consumption) and the depth of the biomedical device. If there are no additional constraints besides the magnetic field safety limit, a near uniform magnetic field can be created through large coils with high currents. However, if size constraints are applied, the optimal coil radius will be at the constraint (i.e., the maximum allowable radius). The current that maximizes the B-field at the implant while not violating the B-field safety constraint at the surface of the skin can be calculated accordingly. In this case, the strength of the maximum achievable magnetic field depends solely on the size constraint. The equations are applicable for the reverse problem as well. Given a minimum needed magnetic field, the necessary coil size and current can be found. Additionally, there

is no benefit to operating with any air gap between the transmitter and the human body due to the nature of the magnetic fields produced by a current loop.

The design rules for an optimal wireless power transmitter given a current constraint differ from the geometrically constrained case. The maximum magnetic field occurs when the current constraint is active. The optimal radius of the transmitter is dependent upon the depth of the medical implant, the magnetic field safety limit, and the current constraint. A critical distance, $Z_{\rm crit}$, was found such that for any implant depths less than $Z_{\rm crit}$, the safety limit constraint is active and the optimal radius is not a function of the implant depth, but only of the current constraint and safety limit. For an implant depth greater than $Z_{\rm crit}$, the safety limit constraint is not active and the optimal radius becomes a linear function of the implant depth.

These design guidelines were experimentally validated and shown to hold true for a constructed case study.

APPENDIX A

A. Nonzero Air Gap With Geometric Constraints

Having the air gap b equal to or nearly equal to zero is the optimal case for maximizing the B-field inside the human body. However, if this distance cannot be made close to zero, the design process proposed in this article can still be utilized with some modifications. For a WPTS that is geometrically constrained, the optimal transmit coil radius is still equal to the constraint limit even if b is non-zero. However, the optimal current in (6) now becomes

$$I = \frac{2B_{\text{safe}} \left(b^2 + R^2\right)^{\frac{3}{2}}}{R^2 \mu}.$$
 (6a)

Increasing the air gap b increases the optimal current, and an increase in b has a larger impact on the optimal current than an increase in the transmit coil radius R.

Additionally, a non-zero air gap causes (8) to change to

$$\Gamma = \frac{\left(b^2 + R^2\right)^{\frac{3}{2}}}{\left(\left(z_{\text{implant}} + b\right)^2 + R^2\right)^{\frac{3}{2}}}.$$
 (8a)

Performing the same substitution as in the *geometrically constrained transmitter optimization* section, and defining a ratio, *a*, the coil radius can be expressed as

$$R = aZ_{\text{implant}}.$$
 (9)

Equation (10) then takes the form

$$\Gamma = \frac{\left(b^2 + a^2 z_{\text{implant}}^2\right)^{\frac{3}{2}}}{\left(\left(z_{\text{implant}} + b\right)^2 + a^2 z_{\text{implant}}^2\right)^{\frac{3}{2}}}.$$
 (10a)

In order to get the same nondimensional insight as (10), another ratio is added for the convenience. If the relationship between the implant depth and the air gap is expressed as $b=c\ z_{\rm implant}$ where c is a non-dimensional ratio, (10a) reduces to

$$\Gamma = \left(\frac{c^2 + a^2}{(c+1)^2 + a^2}\right)^{\frac{3}{2}}.$$
 (10b)

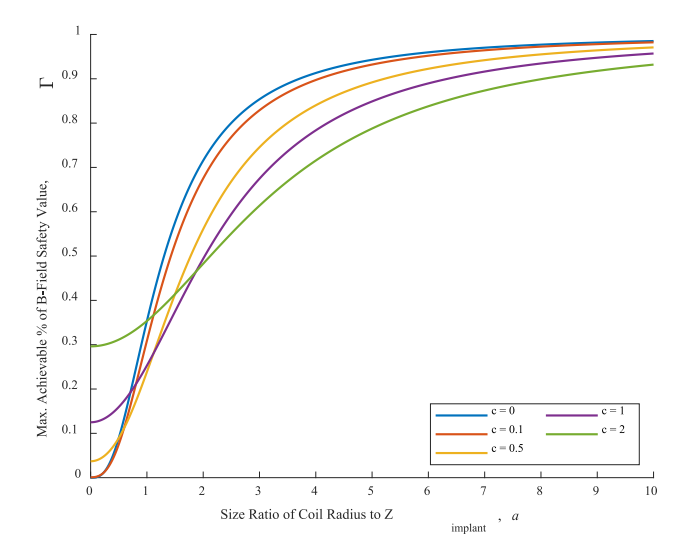


Fig. 12 Maximum achievable B-field ratio (Γ) versus coil radius ratio (a) for different air gaps ($c=b~Z_{implant}$). As the air gap increases (i.e., c increases), the maximum achievable B-field (or equivalently, Γ) decreases for the same a.

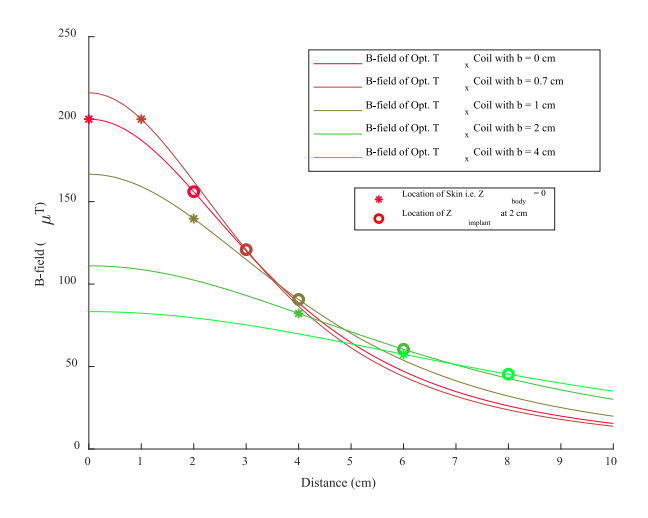


Fig. 13 B-field produced along the centerline of optimal transmit coils in WPTSs with different air gaps b. The implant is located at a depth of 2 cm for all cases and its location for each different WPTS is marked with a circle. The strength of the B-field at the skin for each case is denoted by a star. Current constraint is 15 A and B-field constraint is 200 μ T.

The effect of the air gap is illustrated in Fig. 12. Generally, as the air gap [represented by c in Fig. 12] increases, the maximum achievable B-field decreases for a given size ratio, a. It is important to note that at a radius equal to zero, Γ can be numerically defined but that definition is trivial since there is no transmit coil.

However, there appear to be cases where a < 1 for which a non-zero air gap (c > 0) seems to be beneficial and gives a higher Γ than the case with no air gap (c = 0). For example, see c = 2 in Fig. 13. This phenomenon is closely related to the unconstrained WPTS optimization presented in the *unconstrained wireless* power transmitter optimization section. In that case, the optimal solution is a large coil with high current that produces a uniform magnetic field just under the safety limit. The same effect can, in part, be duplicated by a tiny coil with extremely high current that

results in a near-uniform magnetic field at some short distance (a < 1) away from the coil. These solutions, while valid, may be impractical since they often necessitate kilo-amperes of current in a small (mm or smaller) coil. The same or greater Γ can be achieved by an alternative coil that has a radius greater than the implant depth, i.e., $a \ge 1$, while utilizing a much lower current.

B. Nonzero Air Gap With Current Constraints

Just as in the original case with no air gap, the optimal current is always at the constraint and there are two different solutions for the optimal radius of the transmit coil. However, instead of the implant distance, $Z_{\rm implant}$ only, the determining factor now is a combination of the air gap and $Z_{\rm implant}$. Similarly to $Z_{\rm crit}$, there is a critical air gap $b_{\rm crit}$ in conjunction with $Z_{implant}$, that determines the optimal radius for the transmitter. $b_{\rm crit}$ is attained by solving the following equation:

$$0 = u_0 I \frac{\left(Z_{\text{implant}}^2 + b_{\text{crit}}^2\right)}{\left(b_{\text{crit}}^2 + 2(Z_{\text{implant}} + b_{\text{crit}})^2\right)^{\frac{3}{2}}} - B_{\text{safe}}. \quad (14a)$$

Given the complexity of the equation, numerical methods are more appropriate.

If the WPTS has an air gap $b \geq b_{\rm crit}$, then the optimal radius of the transmit coil is

$$R_{\text{opt}} = \sqrt{2} \left(Z_{\text{implant}} + b \right), \tag{11a}$$

which is similar to (11) (when $Z_{\rm implant} > Z_{\rm crit}$ and b=0). Indeed, the derivation of (11a) is identical to those of (11) and (16), except that $z=Z_{\rm implant} + b$ is substituted into (15) instead of $z=Z_{\rm implant}$.

If $b < b_{\rm crit}$, the optimal radius of the coil $R_{\rm opt}$ is determined by

$$\frac{2(b^2 + R_{\text{opt}}^2)^{\frac{3}{2}} B_{\text{safe}}}{I u_0} - R_{\text{opt}}^2 = 0.$$
 (12a)

Similarly, using numerical methods are the most suitable. The explanation for (11a) and (12a) is identical to the justification for (11) and (12). The optimal coil radius without a magnetic field safety constraint is given by (11a). However, there exists a region, dependent on the air gap and also the implant depth, where using (11a) would cause the magnetic field safety constraint to be violated at the skin. Therefore, in order to avoid this behavior while still maximizing the B-field at the implant, the optimal radius is given in (12a).

These principles are illustrated in Fig. 13, which shows the B-field produced by optimal transmit coils for an implant located 2 cm beneath the skin with differing air gaps. Each WPTS has a current constraint of 15 A and a magnetic field safety constraint of 200 μ T. Using (14a), the critical air gap for the given implant location and constraints is $b_{\rm crit}=1.05$ cm. The first two WPTSs with air gaps equal to 0 and 1 cm are cases where $b < b_{\rm crit}$, which implies that the solution of (12a) is the optimal radius for these WPTSs. It can be observed that the B-field at the skin, marked by a star on the graph, is at the safety limit of 200 μ T for the two WPTSs under consideration. In scenarios when b >

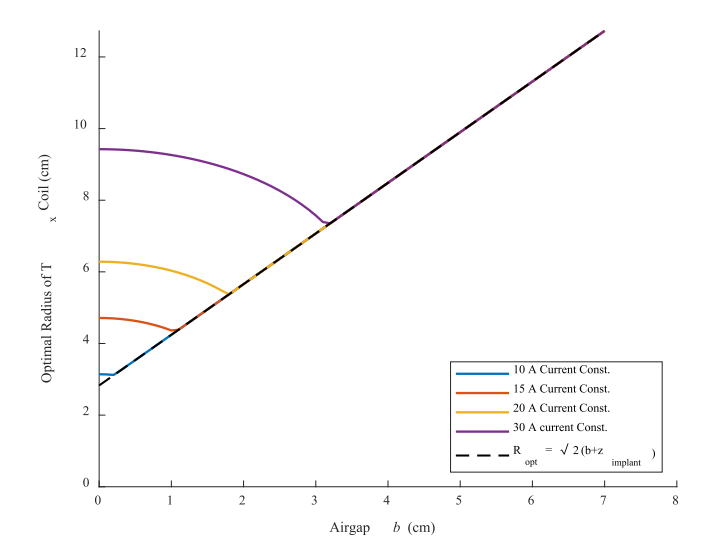


Fig. 14 Optimal radius of transmit coil in terms of different air gaps for various current constrained WPTS. For air gaps below b_{crit} , the optimal radius is polynomic. If the air gaps are greater than b_{crit} , the optimal radius is obtained by (14a), regardless of the current constraint. All WPTSs have a magnetic field safety constraint of 200 μ T and $z_{implant} = 2$ cm.

 $b_{\rm crit}$, the B-field at the skin is no longer at 200 μ T. Moreover, the larger the air gap, the lower the B-field strength is at the implant.

Equation (12a) differs from (12) in that the optimal radius for transmit coils located below the critical distance is not constant, but rather polynomic. Fig. 14 shows the radius of the optimal transmit coil as a function of the air gap b with differing current constraints. The magnetic field safety constraint is set constant at 200 μ T and $z_{\rm implant} = 2$ cm for all systems.

It is essential to note that the critical airgap $b_{\rm crit}$ is a function of current constraint, magnetic field safety limit, and $z_{\rm implant}$. More importantly, there are combinations of constraints and implant depths for which $b_{\rm crit}$ is undefined. This implies that the optimal solution of (11a) will not violate the safety limit regardless of how small the air gap may be.

Furthermore, depending on the imposed constraints, there may be two solutions to (14a) and (12a). However, one of them is nonsensical. In particular, (14a) may have a negative solution for $b_{\rm crit}$ which is invalid since $b_{\rm crit}$ is nonnegative by definition. For (12a), both solutions to the optimal radius are positive however the larger radius is the feasible and preferable optimal radius. The other solution is usually too small, on the order of mm or smaller.

REFERENCES

- H. Jiang et al., "A low-frequency versatile wireless power transfer technology for biomedical implants," *IEEE Trans. Biomed. Circuits Syst.*, vol. 7, no. 4, pp. 526–535, Aug. 2013.
- [2] "Implantable device replacement procedure | Johns Hopkins medicine," 2019, Accessed: Jul.-Oct. 2019. [Online]. Available: https://www.hopkinsmedicine.org/health/conditions-and-diseases/ implantable-device-replacement-procedure
- [3] D. Ahn and M. Ghovanloo, "Optimal design of wireless power transmission links for millimeter-sized biomedical implants," *IEEE Trans. Biomed. Circuits Syst.*, vol. 10, no. 1, pp. 125–137, Feb. 2016.
- [4] J. S. Ho et al., "Wireless power transfer to deep-tissue microimplants.," Proc. Nat. Acad. Sci. USA, vol. 111, no. 22, pp. 7974–7979, Jun. 2014.

- [5] D. Ahn and S. Hong, "Wireless power transmission with self-regulated output voltage for biomedical implant," *IEEE Trans. Ind. Electron.*, vol. 61, no. 5, pp. 2225–2235, May 2014.
- [6] R.-F. Xue, K.-W. Cheng, and M. Je, "High-Efficiency wireless power transfer for biomedical implants by optimal resonant load transformation," *IEEE Trans. Circuits Syst. I Reg. Papers*, vol. 60, no. 4, pp. 867–874, Apr. 2013.
- [7] S. Ha, C. Kim, J. Park, S. Joshi, and G. Cauwenberghs, "Energy recycling telemetry IC with simultaneous 11.5 mW power and 6.78 Mb/s backward data delivery over a single 13.56 MHz inductive link," *IEEE J. Solid-State Circuits*, vol. 51, no. 11, pp. 2664–2678, Nov. 2016.
- [8] Y. Jia, B. Lee, S. A. Mirbozorgi, M. Ghovanloo, W. Khan, and W. Li, "Towards a free-floating wireless implantable optogenetic stimulating system," in *Proc. IEEE 60th Int. Midwest Symp. Circuits Syst.*, 2017, pp. 381–384.
- [9] A. K. RamRakhyani, S. Mirabbasi, and M. Chiao, "Design and optimization of resonance-based efficient wireless power delivery systems for biomedical implants," *IEEE Trans. Biomed. Circuits Syst.*, vol. 5, no. 1, pp. 48–63, Feb. 2011.
- [10] W. X. Zhong, C. Zhang, X. Liu, and S. Y. R. Hui, "A methodology for making a three-coil wireless power transfer system more energy efficient than a two-coil counterpart for extended transfer distance," *IEEE Trans. Power Electron.*, vol. 30, no. 2, pp. 933–942, Feb. 2015.
- [11] H. S. Gougheri and M. Kiani, "Optimal frequency for powering millimetersized biomedical implants inside an inductively-powered homecage," in *Proc. 38th Annu. Int. Conf. IEEE Eng. Med. Biol. Soc.*, 2016, pp. 4804–4807.
- [12] A. Yakovlev, S. Kim, and A. Poon, "Implantable biomedical devices: Wireless powering and communication," *IEEE Commun. Mag.*, vol. 50, no. 4, pp. 152–159, Apr. 2012.
- [13] J. S. Ho, S. Kim, and A. S. Y. Poon, "Midfield wireless powering for implantable systems," *Proc. IEEE*, vol. 101, no. 6, pp. 1369–1378, Jun. 2013.
- [14] Y.-T. Liao, H. Yao, A. Lingley, B. Parviz, and B. P. Otis, "A 3-uW CMOS glucose sensor for wireless contact-lens tear glucose monitoring," *IEEE J. Solid-State Circuits*, vol. 47, no. 1, pp. 335–344, Jan. 2012.
- [15] A. S. Y. Poon, S. O'Driscoll, and T. H. Meng, "Optimal frequency for wireless power transmission into dispersive tissue," *IEEE Trans. Antennas Propag.*, vol. 58, no. 5, pp. 1739–1750, May 2010.
- [16] "International commission on non-ionizing radiation protection icnirp publication-2010 ICNIRP guidelines for limiting exposure to time-varying electric and magnetic fields (1 hz-100 khz) ICNIRP guidelines guidelines for limiting exposure to time-varying el," 2010.
- [17] "International commission on non-ionizing radiation protection ICNIRP guidelines for limiting exposure to electromagnetic fields (100 KHz to 300 GHz)," 2020.
- [18] "C95.1-2019 IEEE Standard for safety levels with respect to human exposure to electric, magnetic, and electromagnetic fields, 0 Hz to 300 GHz," 2019.
- [19] "Radio frequency safety | federal communications commission," 2019, Accessed: Jul. 22, 2019. [Online]. Available: https://www.fcc.gov/general/radio-frequency-safety-0
- [20] Y. Zhou, S. Chul Yang, D. J. Apo, D. Maurya, and S. Priya, "Tunable self-biased magnetoelectric response in homogenous laminates," *Appl. Phys. Lett.*, vol. 101, no. 23, pp. 232905, Dec. 2012.
- [21] S. Dong, J.-F. Li, and D. Viehland, "Longitudinal and transverse magnetoelectric voltage coefficients of magnetostrictive/piezoelectric laminate composite: Experiments," *IEEE Trans. Ultrason. Ferroelect. Freq. Control*, vol. 51, no. 7, pp. 794–799, Jul. 2004.
- [22] J. Ryu et al., "Ubiquitous magneto-mechano-electric generator," Energy Environ. Sci., vol. 8, no. 8, pp. 2402–2408, Jul. 2015.
- [23] T. Nan et al., "Acoustically actuated ultra-compact NEMS magnetoelectric antennas," Nat. Commun., vol. 8, no. 1, pp. 1–8, Dec. 2017.
- [24] T. Rupp, B. D. Truong, S. Williams, and S. Roundy, "Magnetoelectric transducer designs for use as wireless power receivers in wearable and implantable applications," *Materials (Basel)*, vol. 12, no. 3, pp. 512–530, Feb. 2019.
- [25] G. Rizzo, V. Loyau, R. Nocua, J. C. Lourme, and E. Lefeuvre, "Potentiality of magnetoelectric composites for wireless power transmission in medical implants," in *Proc. 13th Int. Symp. Med. Inf. Commun. Technol.*, 2019, pp. 1–4.
- [26] K. Malleron, A. Gensbittel, H. Talleb, and Z. Ren, "Experimental study of magnetoelectric transducers for power supply of small biomedical devices," *Microelectron. J*, vol. 88, no. 11, pp. 184–189, Jun. 2019.

- [27] R. C. O'Handley, J. K. Huang, D. C. Bono, and J. Simon, "Improved wireless, transcutaneous power transmission for in vivo applications," IEEE Sens. J., vol. 8, no. 1, pp. 57-62, Jan. 2008.
- [28] J. Xu et al., "A low frequency mechanical transmitter based on magnetoelectric heterostructures operated at their resonance frequency," Sensors, vol. 19, no. 4, pp. 853-866, Feb. 2019.
- [29] B. D. Truong and S. Roundy, "Experimentally validated model and power optimization of a magnetoelectric wireless power transfer system in free-free configuration," Smart Mater. Struct., vol. 29, no. 8, Aug. 2020, Art. no. 085053.
- [30] B. D. Truong, E. Andersen, C. Casados, and S. Roundy, "Magnetoelectric wireless power transfer for biomedical implants: Effects of non-uniform magnetic field, alignment and orientation," Sensors Actuators A Phys., vol. 316, Aug. 2020, Art. no. 112269.
- [31] B. H. Waters, A. P. Sample, P. Bonde, and J. R. Smith, "Powering a ventricular assist device (VAD) with the free-range resonant electrical energy delivery (FREE-D) System," Proc. IEEE, vol. 100, no. 1, pp. 138-149, Jan. 2012.
- [32] S. W. Park, "Investigating human exposure to a practical wireless power transfer system using and the effect about key parameters of dosimetry," PloS One, vol. 15, no. 8, Aug. 2020, Art. no. e0236929.
- [33] M. A. Tanha, F. Fahimi Hanzaee, R. Bayford, and A. Demosthenous, "RF wireless power transfer for EIT neonate lung function monitoring," in Proc. IEEE Int. Symp. Circuits Syst., 2021, pp. 1-5.
- [34] J. J. Abbott and B. Osting, "Optimization of coreless electromagnets to maximize field generation for magnetic manipulation systems," IEEE Magn. Lett., vol. 9, 2018, Art. no. 1300104.
- [35] R. Ravaud, G. Lemarquand, V. Lemarquand, S. Babic, and C. Akyel, "Calculation of the magnetic field created by a thick coil," J. Electromagn. Waves Appl., vol. 24, no. 10, pp. 1405-1418, 2010.
- [36] E. Andersen, B. D. Truong, and S. Roundy, "Optimal coil design for wireless powering of biomedical implants considering safety constraints," in Proc. IEEE MTT-S Wireless Power Transfer Conf., 2019, pp. 106-110.
- [37] I. Marinova and V. Mateev, "Electromagnetic field modeling in human tissue," *Physics*, vol. 4, no. 4, pp. 140–145, 2010.
 [38] P. K. Sharma and S. K. Guha, "Transmission of time varying magnetic field
- through body tissue," J. Biol. Phys., vol. 3, no. 2, pp. 95-102, Jun. 1975.
- [39] P. N. Morgan, "Optimal design and construction of a lightweight minimum-power solenoid magnet," IEEE Trans. Magn., vol. 37, no. 5, pp. 3814-3817, Sept. 2001.
- [40] A. Miklavc, "The solenoid which gives the desired value of magnetic field for the smallest possible volume of conductor," J. Appl. Phys., vol. 45, no. 4, pp. 1680-1681, Apr. 1974.
- [41] P. N. Murgatroyd, "The optimal form for coreless inductors," IEEE Trans. Magn., vol. 25, no. 3, pp. 2670-2677, May 1989.

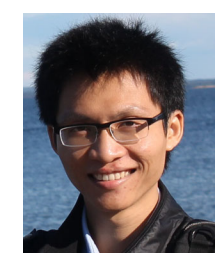


Erik Andersen received the B.Sc. and Masters of Mechanical Engineering degrees in 2018 from the University of Utah, Salt Lake City, UT, USA, where he is currently working toward the Ph.D. degree with the Department of Mechanical Engineering under Dr.

His research interests include wireless power transfer (specifically for implantable biomedical devices), system design and optimization, and magnetoelectric transducers



Curtis Casados received the B.S. degree in mechanical engineering from the University of Utah, Salt Lake City, UT, USA, in 2020. He is currently working toward the M.S. degree in computer science with the University of Southern California, Los Angeles, CA,



Binh Duc Truong received the B.E. degree in mechatronics from the Ho Chi Minh City University of Technology, Ho Chi Minh City, Vietnam, in 2012, the M.Sc. degree in microsystem and nanosystem technology from the Buskerud and Vestfold University College, Norway, in 2015, and the Ph.D. degree in mechanical engineering from the University of Utah, Salt Lake City, UT, USA, in 2020.

His research interest includes electromagnetics, energy harvesting and wireless power transfer



Shad Roundy (Member, IEEE) received the M.S. and Ph.D. degrees in mechanical engineering from the University of California at Berkeley, Berkeley, CA, USA, in 2000 and 2003, respectively.

From 2003 to 2005, he was a Lecturer with Australian National University. From 2005 to 2012, he was with the MEMS industry, developing tire pressure sensors, accelerometers, gyroscopes, and energy harvesters. In 2012, he was the Faculty with the University of Utah, where he is currently an Associate Professor with the Department of Mechanical

Engineering. His research interests include energy harvesting, wireless power transfer, and more generally MEMS sensors and actuators